RESEARCH ARTICLE

# Quinazoline-2,4(1H,3H)-dione derivatives as new class of CB1 Agonists: A pharmacophore-based virtual screening workflow and Lead discovery

[version 1; peer review: 2 approved]

Abdellah EL AISSOUQ[1], MOURAD STITOU[1], Mohamed Enneiymy[2], Said El Rhabori[1], Hicham Zaitan[1], Abdelkrim Ouammou[3], Fouad Khalil[1]

[1]Universite Sidi Mohamed Ben Abdellah Faculte des Sciences et Techniques de Fes, Fes, Fes-Boulemane, Morocco
[2]Universite Ibn Zohr Faculte des Sciences Agadir, Agadir, Souss-Massa-Draa, Morocco
[3]Universite Sidi Mohamed Ben Abdellah Faculte des Sciences Dhar El Mahraz-Fes, Fes, Fes-Boulemane, Morocco

**v1** **First published:** 27 Nov 2025, **14**:1322
https://doi.org/10.12688/f1000research.171433.1
**Latest published:** 27 Nov 2025, **14**:1322
https://doi.org/10.12688/f1000research.171433.1

## Abstract

### Background

The cannabinoid 1 (CB1) receptor is the primary target of $\Delta^9$-tetrahydrocannabinol ($\Delta^9$-THC), the psychoactive component of cannabis sativa (commonly known as “kif” in Morocco).

### Methods

Here, we identified novel CB1 agonists using virtual screening approaches. First, we developed a pharmacophore model based on the known CB1 agonist AM11542 and screened a database of over three million compounds. Molecular docking using AutoDock Vina identified 61 hits with binding affinities of less than -9.00 Kcal/mol. Subsequent ADME-Tox (absorption, distribution, metabolism, excretion, and toxicity) analysis narrowed the selection to 18 promising candidates.

### Results

Among these, three agonists exhibited strong characteristics, including a favorable inhibition constant (Ki) and key hydrogen-bond interactions with critical residues in the CB1 binding pocket: PUBChem157251136 (Ki=2.09 nM), ZINC64438485 (Ki= 0.262 nM) and ZINC64438506 (Ki =0.244 nM). These agonists formed stable hydrogen

**Open Peer Review**

**Approval Status** ✓ ✓

| | 1 | 2 |
|---|---|---|
| **version 1** 27 Nov 2025 | ✓ view | ✓ view |

1. **Fatima En-nahli**, University of Moulay Ismail, Meknes, Morocco

2. **Mourad Fawzi**, Laboratory of Molecular Chemistry, Marrakech, Morocco

Any reports and responses or comments on the article can be found at the end of the article.

bonds with CB1 binding pocket residues (Ser383, Ser173, His178 and Thr197). Molecular dynamics simulations (100 ns, GROMACS) demonstrated structural stability (RMSD < 1 nm) and low conformational flexibility (RMSF < 1 nm) for all complexes. MM-GBSA binding free energy calculations further confirmed the thermodynamic stability of all complexes, with interaction energies ranging from -30.59 to -49.98 kcal/mol. These comprehensive simulations confirm that all identified agonist complexes maintain stable binding conformations with optimal interaction profiles characteristic of CB1 receptor activation.

**Conclusion**

These results could pave the way for researching and developing new quinazolinz-2, 4(1H, 3H)-Dione derivatives as a new class of CB1 receptor agonists.

**Keywords**
CB1 agonists, pharmacophore based virtual screening, lead discovery, quinazoline-2, 4(1H, 3H)-dione derivatives

This article is included in the Cheminformatics gateway.

**Corresponding author:** Abdellah EL AISSOUQ (abdellah.elaissouq@usmba.ac.ma)

**Author roles: EL AISSOUQ A**: Methodology, Writing – Original Draft Preparation, Writing – Review & Editing; **STITOU M**: Investigation, Methodology, Validation, Visualization; **Enneiymy M**: Methodology, Supervision, Validation, Visualization; **El Rhabori S**: Methodology, Resources, Software, Validation; **Zaitan H**: Data Curation, Supervision, Validation, Visualization; **Ouammou A**: Data Curation, Investigation, Methodology, Validation; **Khalil F**: Methodology, Supervision, Validation, Visualization

**Competing interests:** No competing interests were disclosed.

**Grant information:** The author(s) declared that no grants were involved in supporting this work.



**How to cite this article:** EL AISSOUQ A, STITOU M, Enneiymy M *et al.* **Quinazoline-2,4(1H,3H)-dione derivatives as new class of CB1 Agonists: A pharmacophore-based virtual screening workflow and Lead discovery [version 1; peer review: 2 approved]** F1000Research 2025, **14**:1322 https://doi.org/10.12688/f1000research.171433.1

**First published:** 27 Nov 2025, **14**:1322 https://doi.org/10.12688/f1000research.171433.1

## I. Introduction

Cannabinoid receptors are classified as G protein-coupled receptors which belong to a family known as the endocannabinoid system, a master regulator of numerous physiological pathways throughout the human body.[1] There are two categories of cannabinoid receptors, known as CB1 and CB2. The CB1 receptor is found throughout multiple organs of the body; it is present in the digestive tract, liver, pancreas, and musculature, in addition to its primary site of localization being in the brain.[2] In fact, CB1 is the most highly expressed receptor in the brain relative to other receptors examined, possessing 7 transmembrane domains with G protein coupling. The CB1 receptor mediates cannabinoid-induced psychotropic effects. The CB2 receptor is more so located within immune cells, where it exerts its immunomodulatory role.

Cannabinoids are a class of chemical compounds which are championed globally for their psychoactive and physiologic whole body functions; for at least 5,000 years,[3,4] mankind has been able to capitalize on the value of cannabinoids. One such natural source of cannabinoids is cannabis, known as "kif" in Moroccan culture, a natural product with a plethora of phytoconstituents including Δ9-tetrahydrocannabinol (THC). The phytochemical THC exerts its psychotropic effects by acting at the CB1 receptor, which also serves as the primary receptor for the endogenous endocannabinoids anandamide (AEA) and 2 arachidonoylglycerol (2-AG).[5] Activation of the CB1 receptor upregulates potassium channel currents and calcium ion channel polarization, making receptor signaling dose dependent and responsive to treatment with pertussis toxin.[6] In addition, CB1 can exist as a homodimer and/or form complexes as heterodimers or heterooligomers with other GPCRs. Lastly, the CB1 receptor is in a complex with GABAergic and glutamatergic cells, and therefore, CB1 receptor stimulation decreases release from GABAergic and glutamatergic cells.[7]

The structural complexes of the cannabinoid receptor CB1 with THC analogs are an important topic of research to help us understand the molecular interactions that underlie cannabinoid signaling. Thus far, the repertoire of known complexes of the CB1 receptor includes the structure of CB1, bound to AM8411,[8] CP55940[9] and AM11542[10] (Figure 1). These structures have a resolution of 2.8-3.4 Å and provide a highly informative account of the binding modes and associated conformational changes that can accompany receptor activation. Several important interacting residues have been found to be conserved between agonist-bound structures, including hydrophobic interactions with LEU193$^{3.29}$, VAL196$^{3.32}$, PHE200$^{3.36}$, TYR275$^{5.39}$, LEU276$^{5.40}$, TRP279$^{5.43}$, TRP356$^{6.48}$, LEU359$^{6.51}$ and MET363$^{6.55}$.[11] These observations further emphasize the importance of these residues in their role of stabilizing binding of agonists to the receptor, while also promoting receptor activation.

There were also three structures solved by means of cryo-electron microscopy (cryo-EM) that included full active states along with the Gi1-2 G protein subunit.[12] The AM11542 CB1 complex is a crystalline structure and had a fusion protein, flavodoxin, which contributes to stabilization of TM6 in an active confirmation.[11] All of the structural coordinates cover the full CB1 protein sequence, covering anywhere between approximately 58% and 62% of each residues in all active structures.[8] The fact that the coordinates do not cover the full sequence is most likely do to the flexibility imparted by both the N and C-terminus and the long ICL3. These structural descriptions not only allow constructs for determining the molecular mechanisms for THC analog activation of the CB1 receptor but also create opportunities for future studies.

In recent years the harmonization of approaches have created several avenues to create CB1 receptor agonists with less adverse effects. This study will previously develop a CB1 agonist pharmacophore model that was used as a virtual screening tool for unique/novel class of CB1 agonists. Using the pharmacophore this was able to screen over 300 million hits, of compounds, parsed from 11 different databases and were able to identify many candidates that have not been screen for cannabinoid receptor binding assay. This highlights the usefulness of computational strategies to find novel therapeutics that have the potential to provide safer alternatives.

## II. Materials and method

### 1. Pharmacophore modeling and virtual screening

Pharmacophore based virtual screening were performed using the Pharmit web interface (http://pharmit.csb.pitt.edu/), which has a number of built-in databases that provide access to comprehensive data; Molprot (4,742,020 molecules), ChEMBL34 (2,264,112 molecules), ZINC (13,127,550 molecules), ChemDiv (1,456,120 molecules), ChemSpace (50,181,678 molecules), Enamine (4,117,328 molecules), MCULE (39,843,637 molecule), MCULE-ULTIMATE (126,471,502 molecules), NCI Open Chemical Repository (52,237 molecules), LabNetwork (1,794,286 molecules), and PubChem (103,302,052 molecules). The pharmacophore model was constructed using selected PDB code 5XRA from the RCSB Protein Data Bank (http://www.rcsb.org/structure/5xra), with agonist AM11542. The model utilized a pharmacophore framework built on five features, adhering to the default parameters of the Pharmit server. The Pharmit filters were applied based on the Lipinski rule of five and Veber's rule to refine the screening process and identify the most selective CB1 agonist. Figure 2 illustrates the multi-step virtual screening process used in this work.

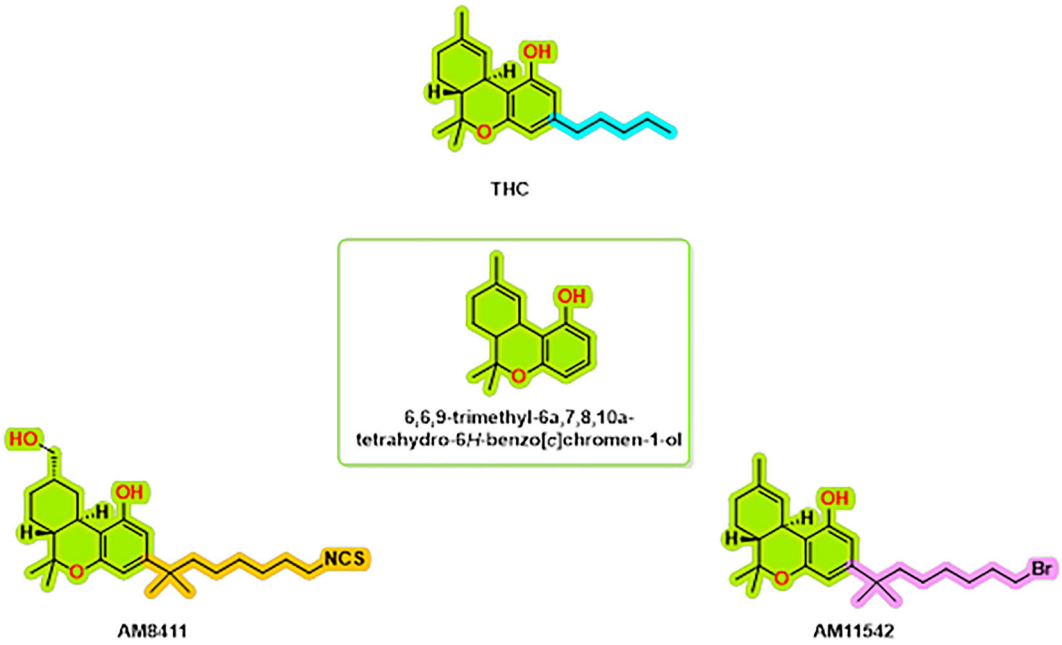


**Figure 1. CB1 receptor agonist chemical structures.**

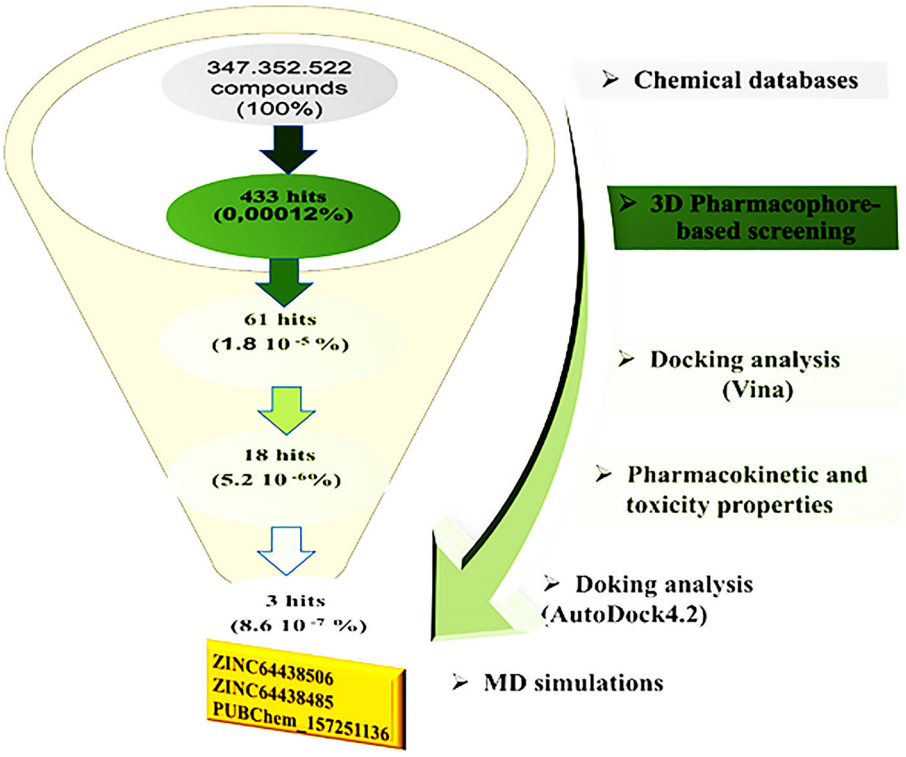


**Figure 2. General workflow used in the present study for identifying new CB1 agonists.**

## 2. ADMET profiling

The ADMET (Absorption, Distribution, Metabolism, Excretion, and Toxicity) filter is one of the phases of the drug discovery and development process.[13–15] This allows researchers to determine potentially druggable drug-like properties and toxicology early on to assess which compounds will be effective drugs with safety potential. Thus, relative to virtual screening, such a filter can detect adverse properties that would fail at much later stages, such as insufficient absorption,

excessive toxicity, and/or suboptimal bioavailability. Two of the trusted websites relied upon to evaluate such properties based upon lipophilicity, logP, solubility, etc., are SwissADME (http://www.swissadme.ch) and pKCSM (https://biosig.lab.uq.edu.au/pkcsm/prediction). Therefore, when these are filtered out early on, time and costs will be effectively saved down the line.

### 3. Molecular docking studies

To estimate the binding affinities of the 433 highest-ranked compounds to CB1, molecular docking was carried out using AutoDock Vina integrated within the PyRx platform. The crystal structure of CB1 (PDB ID: 5XRA), with a resolution of 2.8 Å,[8,16,17] was retrieved from the Protein Data Bank. Before docking, water molecules and the native ligand were removed from the protein, followed by the addition of polar hydrogen atoms and Kollman charges. The prepared protein structure was then energy-minimized using UCSF Chimera and saved in PDBQT format.

Prior to docking, all 433 compounds underwent pre-optimization utilizing the Universal Force Field (UFF) in combination with the conjugate gradient algorithm.[18] Optimization parameters were set to 2000 total steps, with updates occurring every step, and the process was programmed to terminate once the energy difference fell below 0.01 kcal/mol.[19] After optimization, the compounds were converted to PDBQT format and docked at specific binding site coordinates (x = -42.052, y = -164.338, z = 306.631). Molecules demonstrating the lowest binding energies and root-mean-square deviation (RMSD) values below 2 Å were selected for subsequent analyses.

### 4. Molecular dynamics simulations

Molecular dynamics (MD) simulations were carried out on the top-ranked docking conformations using the GROMACS 2024.4 software package, employing the CHARMM27 all-atom force field.[20] The topology files for the CB1 receptor were generated using the pdb2gmx tool,[21] while the ligand topologies were prepared through the CHARMM General Force Field (CGenFF) using the Param-Chem server.[22–24] Each receptor-ligand complex was embedded in a triclinic simulation box and solvated with TIP3P water molecules, maintaining a minimum distance of 1.0 nm from the box boundaries. To neutralize the systems, $Na^+$ and $Cl^-$ ions were added accordingly.

Prior to the production runs, energy minimization was performed using the steepest descent algorithm for 50,000 steps to eliminate steric clashes and ensure system stability. Subsequently, two equilibration phases were conducted: first under the NVT ensemble to stabilize temperature, followed by the NPT ensemble to equilibrate pressure and density. Input files for both equilibration and production stages were customized to adjust parameters such as trajectory-saving intervals, energy monitoring, and other essential simulation settings. Finally, each ligand-receptor system underwent 100 ns of production MD simulation at a constant temperature of 300 K, pressure of 1 bar, and a time step of 2 femtoseconds.

### 5. MM/GBSA method

The binding free energy was calculated via MM/GBSA (Molecular Mechanics Generalized Born Surface Area).[25] This approach utilizes force fields of molecular mechanics and an implicit solvent approach to conclude stability and binding tendencies of molecular complexes. It is particularly useful for classifying ligands and understanding overall energetic contributions of molecular recognition. The binding free energy ΔGbind of a complex can be calculated as follows:

$$\mathbf{\Delta G_{bind} = \Delta E_{MM} + \Delta G_{solv} - T\Delta S} \quad \text{(Eq.1)}$$

Where:

$$\mathbf{\Delta E_{MM}} = E_{MM}^{complex} - \left(E_{MM}^{receptor} + E_{MM}^{ligand}\right) \quad \text{(Eq.2)}$$

$$\mathbf{\Delta G_{solv}} = G_{solv}^{complex} - \left(G_{solv}^{receptor} + G_{solv}^{ligand}\right) \quad \text{(Eq.3)}$$

$$\mathbf{G_{solv} = G_{GB} + G_{SA}}$$

Where $T\Delta S$, $\Delta E_{MM}$ and $\Delta G_{sol}$ are the conformational entropy upon binding, the changes of the gas phase molecular mechanism (MM) energy and the solvation free energy, respectively.

## III. Results and discussion

### 1. Pharmacophore

The pharmacophore model of the CB1 receptor agonist was generated based on the AM11542 agonist. The results are shown in Figure 3. A five-point model with 1 aromatic, 2 hydrogen bond acceptors and 2 hydrophobic regions was generated using the Pharmit web server.[26]

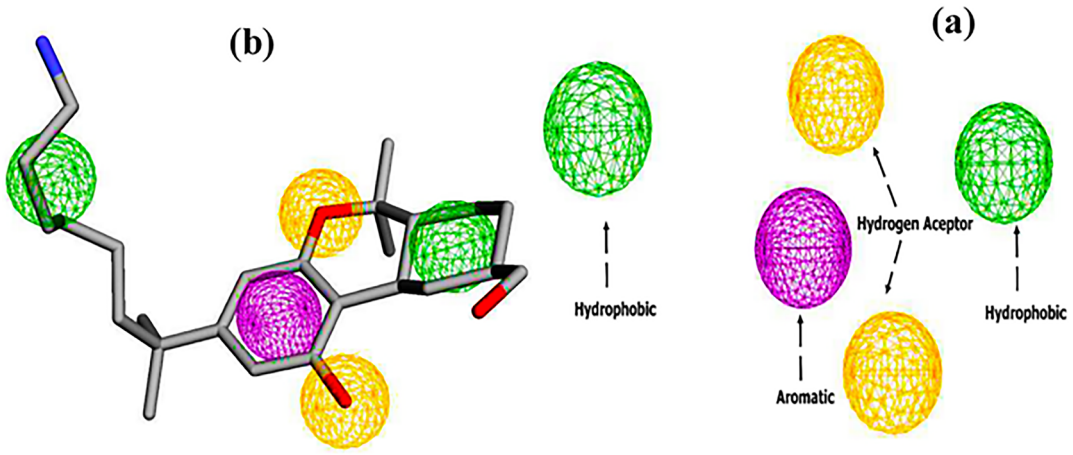


**Figure 3. Pharmacophore features (a) two hydrogen bond acceptors (2HBA, yellow color), two hydrophobic groups (2HY, Green color), and one aromatic group (1AR, purple color), (b) Pharmacophore feature mapping of AM11542 agonist.**

Subsequently, virtual screening was performed across 11 databases, identifying 433 compounds containing molecular groups that matched the pharmacophore mode.

## 2. Virtual screening

Pharmacophore-based virtual screening was performed using information from the previous pharmacophore model. Approximately 300 million compounds from the Pharmit database were filtered. The criteria for filtering the library were as follows: molecular weight limits were set at 250-500 Da, the maximum number of hydrogen bond donors was less than 4, the maximum number of hydrogen bond acceptors was less than 9, the maximum number of rotatable bonds was less than 9, Log P was between 2 and 5, and polar surface area was less than 140 Å. The results are computed and classified according to different criteria such as energy minimization. The 433 top-ranked compounds are presented in Table 1.

Next, molecular docking analysis was performed using AutoDock Vina, implemented in the PyRx software. Compounds with a binding affinity of less than - 9.00 kcal/mol were selected for further analysis, while the others were excluded. Additionally, the predicted binding modes were required to have a root-mean-square deviation (RMSD) of less than 2Å when superimposed onto the native agonist (AM11542). The top 61 selected compounds are listed in Table 2, while the remaining candidates are provided in **Table S1** (see supplementary data).

**Table 1. Pharmacophore-based virtual screening of compounds from 11 databases on the Pharmit server.**

| Pharmit database | Molecules | Hits |
|---|---|---|
| Molprot | 4,742,020 | **58** |
| ChEMBL34 | 2,264,112 | **134** |
| ZINC | 13,127,550 | **32** |
| ChemDiv | 1,456,120 | **76** |
| ChemSpace | 50,181,678 | **0** |
| Enamine | 4,117,328 | **5** |
| MCULE | 39,843,637 | **23** |
| MCULE-ULTIMATE | 126,471,502 | **0** |
| NCI Open Chemical Repository | 52,237 | **0** |
| LabNetwork | 1,794,286 | **63** |
| PubChem | 103,302,052 | **42** |
| **Total** | **347.352.522** | **433** |

**Table 2. Top 61 compounds selected based on docking binding affinity (binding affinity < -9.00 Kcal/mol) and rmsd (rmsd < 2 Å) values.**

| Code | Binding affinity (Kcal/mol) | rmsd | Code | Binding affinity (Kcal/mol) | rmsd |
|---|---|---|---|---|---|
| ZINC35377792 | -10.526 | 1.766 | ZINC21525754 | -9.349 | 1.086 |
| ZINC17286185 | -10.487 | 1.825 | ZINC35377780 | -9.311 | 1.265 |
| ZINC45898833 | -10.415 | 1.964 | PubChem-16352732 | -9.308 | 0.823 |
| ZINC35562518 | -10.410 | 1.055 | PubChem-136659176 | -9.294 | 1.082 |
| ZINC35377809 | -10.202 | 1.239 | PubChem-135405892 | -9.292 | 1.457 |
| ZINC64438506 | -10.189 | 1.395 | PubChem-126853168 | -9.271 | 1.275 |
| PubChem-156469643 | -10.074 | 1.867 | PubChem-25220434 | -9.254 | 1.924 |
| PubChem-89734004 | -10.054 | 1.291 | ZINC20138980 | -9.240 | 1.274 |
| PubChem-50762870 | -10.049 | 1.717 | ZINC169 | -9.236 | 1.227 |
| PubChem-86747888 | -10.035 | 1.776 | ZINC96385691 | -9.222 | 1.955 |
| ZINC45899482 | -10.006 | 1.796 | ZINC65196494 | -9.217 | 0.750 |
| ZINC64438485 | -9.944 | 1.964 | MolPort-009-386-250 | -9.208 | 1.702 |
| PubChem-121231416 | -9.858 | 1.197 | PubChem-41119771 | -9.192 | 1.542 |
| ZINC21797190 | -9.850 | 1.617 | ZINC20113894 | -9.173 | 0.794 |
| ZINC45899726 | -9.828 | 1.718 | ZINC20113894 | -9.173 | 0.794 |
| ZINC45900106 | -9.824 | 1.499 | ZINC35377767 | -9.130 | 1.670 |
| PubChem-53794837 | -9.820 | 1.352 | PubChem-71600230 | -9.127 | 1.653 |
| ZINC45899547 | -9.785 | 1.651 | ZINC45899386 | -9.127 | 1.416 |
| CHEMBL1652254 | -9.763 | 1.547 | ZINC35377767 | -9.121 | 1.351 |
| ZINC2245716 | -9.652 | 1.160 | ZINC13365292 | -9.100 | 1.219 |
| ZINC45900103 | -9.615 | 1.977 | LN00379431 | -9.098 | 1.083 |
| ZINC35377763 | -9.518 | 1.176 | PubChem-3750748 | -9.095 | 1.627 |
| PUBChem 157251136 | -9.492 | 1.362 | ZINC4034881 | -9.089 | 1.300 |
| ZINC09598984 | -9.489 | 1.654 | ZINC65196500 | -9.068 | 1.934 |
| ZINC35377731 | -9.485 | 1.417 | ZINC100771598 | -9.068 | 1.445 |
| ZINC 35377767 | -9.465 | 1.474 | PubChem-25352696 | -9.067 | 1.172 |
| ZINC 21723065 | -9.463 | 1.471 | PubChem-91428044 | -9.045 | 1.614 |
| PubChem-42810820 | -9.454 | 1.742 | ZINC35377731 | -9.034 | 1.382 |
| ChemDiv-C260-2692 | -9.424 | 1.461 | ZINC33057775 | -9.027 | 1.058 |
| PubChem-135869534 | -9.413 | 1.985 | ZINC96385592 | -9.010 | 1.069 |
| PubChem-91487881 | -9.353 | 1.714 | | | |

## 3. Toxicity filters

The ranked compounds from docking analysis were evaluated for potential toxicity, including an AMES toxicity test, an acute oral toxicity test in rats ($LD_{50}$), a skin sensitization test and a maximum tolerated dose analysis. Highly toxic compounds are not considered in further studies. The top selected compounds are presented in Table 3. The other are presented in the supplementary data (**Table S2).**

As described in Table 3, all selected compounds exhibited no Skin Sensitisation and no AMES toxicity. Additionally, the $LD_{50}$ values for oral rat toxicity, ranging from 1.439 to 3.354 mol/kg, suggest moderate acute toxicity levels, consistent with safety margins suitable for therapeutic use. Moreover, the maximum tolerated dose in humans' ranges from -1.12 to 1.059 Log mg/kg/day.

**Table 3. *In silico* prediction of Skin Sensitisation.** AMES toxicity, oral rat acute toxicity ($LD_{50}$), and Max Tolerated dose in humans.

| Code | Skin Sensitisation | AMES toxicity | Oral Rat Acute Toxicity ($LD_{50}$ (mol/kg)) | Max. tolerated dose (human) (Log mg/kg/day) |
|---|---|---|---|---|
| ZINC35377792 | No | No | 2.785 | 0.412 |
| ZINC17286185 | No | No | 2.474 | 0.222 |
| ZINC45898833 | No | No | 2.617 | 0.328 |
| ZINC35562518 | No | No | 2.441 | 0.215 |
| ZINC64438506 | No | No | 2.744 | 0.685 |
| PubChem-156469643 | No | No | 2.904 | -1.12 |
| PubChem-89734004 | No | No | 3.02 | -0.825 |
| PubChem-86747888 | No | No | 3.001 | -0.913 |
| ZINC64438485 | No | No | 2.816 | 0.381 |
| PubChem-121231416 | No | No | 2.818 | -0.595 |
| ZINC21797190 | No | No | 3.085 | 0.61 |
| ZINC45899726 | No | No | 2.748 | 0.647 |
| PubChem-53794837 | No | No | 2.569 | -0.725 |
| CHEMBL1652254 | No | No | 3.004 | 0.428 |
| ZINC2245716 | No | No | 2.469 | 0.586 |
| PUBChem 157251136 | No | No | 2.812 | -0.095 |
| Zinc35377731 | No | No | 2.863 | 0.328 |
| Zinc21723065 | No | No | 2.544 | 0.463 |
| PubChem-42810820 | No | No | 2.73 | 0.562 |
| ChemDiv-C260-2692 | No | No | 2.475 | 0.6 |
| PubChem-135869534 | No | No | 3.077 | 0.604 |
| PubChem-91487881 | No | No | 2.433 | -0.088 |
| ZINC21525754 | No | No | 2.753 | -0.134 |
| PubChem-16352732 | No | No | 2.218 | 0.971 |
| PubChem-136659176 | No | No | 2.242 | 0.572 |
| PubChem-135405892 | No | No | 3.075 | 0.607 |
| PubChem-126853168 | No | No | 2.67 | 0.443 |
| ZINC65196494 | No | No | 3.354 | -0.164 |
| PubChem-41119771 | No | No | 2.38 | 0.016 |
| ZINC20113894 | No | No | 2.574 | 0.429 |
| ZINC20113894 | No | No | 2.574 | 0.429 |
| PubChem-71600230 | No | No | 2.048 | 0.395 |
| ZINC13365292 | No | No | 2.604 | 0.134 |
| LN00379431 | No | No | 2.567 | 0.663 |
| PubChem-3750748 | No | No | 3.038 | -0.137 |
| ZINC4034881 | No | No | 2.576 | 0.549 |
| ZINC65196500 | No | No | 3.156 | -0.141 |
| ZINC100771598 | No | No | 3.008 | 0.471 |
| PubChem-25352696 | No | No | 2.552 | 1.059 |
| PubChem-91428044 | No | No | 1.439 | 0.563 |
| ZINC35377731 | No | No | 2.863 | 0.328 |
| ZINC33057775 | No | No | 2.503 | 0.769 |

## 4. Physicochemical properties and bioavailability

Physicochemical properties were evaluated using Lipinski's rule of five,[27] Ghose's rule,[28] Veber's rule,[29] Egan's rule[30] and Muegge's rule,[31] with results detailed in Table 4. Based on these guidelines, it is suggested that for a compound to be effectively absorbed and administered orally, it must meet specific physicochemical parameters. These criteria serve as essential benchmarks for assessing the compound's potential for bioavailability and oral absorption. Compounds with two or more violations are not considered in the further analysis (see **Table S3** in supplementary data).

**Table 4. Physico-chemical properties based on the rules of Lipinski, Ghose, Veber, Egan and Muegge for the highest ranked compounds.**

| Code | Lipinski #violations | Ghose #violations | Veber #violations | Egan #violations | Muegge #violations |
|---|---|---|---|---|---|
| ZINC17286185 | 0 | 1 | 0 | 0 | 0 |
| ZINC35562518 | 0 | 1 | 0 | 0 | 0 |
| ZINC64438506 | 0 | 1 | 0 | 0 | 0 |
| PubChem-156469643 | 0 | 0 | 0 | 0 | 1 |
| PubChem-89734004 | 0 | 0 | 0 | 0 | 0 |
| PubChem-86747888 | 0 | 0 | 0 | 0 | 1 |
| ZINC64438485 | 0 | 1 | 0 | 0 | 0 |
| PubChem-121231416 | 0 | 0 | 0 | 0 | 0 |
| ZINC21797190 | 0 | 0 | 0 | 0 | 0 |
| PubChem-53794837 | 0 | 0 | 0 | 0 | 1 |
| CHEMBL1652254 | 0 | 0 | 0 | 0 | 1 |
| PUBChem 157251136 | 0 | 0 | 0 | 0 | 0 |
| PubChem-42810820 | 0 | 0 | 0 | 0 | 0 |
| ChemDiv-C260-2692 | 1 | 1 | 0 | 0 | 0 |
| PubChem-135869534 | 0 | 0 | 0 | 0 | 0 |
| PubChem-91487881 | 0 | 0 | 0 | 0 | 0 |
| ZINC21525754 | 0 | 0 | 0 | 0 | 0 |
| PubChem-16352732 | 0 | 0 | 0 | 0 | 0 |
| PubChem-136659176 | 0 | 1 | 1 | 1 | 1 |
| PubChem-135405892 | 0 | 0 | 0 | 0 | 0 |
| PubChem-126853168 | 1 | 0 | 0 | 0 | 0 |
| ZINC65196494 | 0 | 0 | 0 | 0 | 0 |
| PubChem-41119771 | 1 | 1 | 0 | 0 | 1 |
| ZINC20113894 | 0 | 0 | 0 | 0 | 0 |
| PubChem-71600230 | 0 | 0 | 0 | 0 | 1 |
| ZINC13365292 | 0 | 0 | 1 | 1 | 0 |
| LN00379431 | 0 | 0 | 0 | 0 | 0 |
| PubChem-3750748 | 1 | 1 | 0 | 0 | 1 |
| ZINC4034881 | 0 | 0 | 0 | 0 | 0 |
| ZINC65196500 | 0 | 0 | 0 | 0 | 0 |
| ZINC100771598 | 0 | 0 | 0 | 0 | 0 |
| PubChem-25352696 | 0 | 0 | 0 | 0 | 0 |
| PubChem-91428044 | 0 | 0 | 0 | 0 | 0 |
| ZINC33057775 | 0 | 0 | 0 | 0 | 0 |

## 5. Pharmacokinetic proprieties

To predict the pharmacokinetic properties of absorption, distribution, metabolism and excretion (ADME), pkCSM web server was used to calculate the following parameters: water solubility (log mol/L), Caco-2 cell permeability, human intestinal absorption (HIA), blood-brain barrier (BBB) permeability, central nervous system (CNS) permeability and total clearance.

Water solubility (LogS) indicates the solubility of a compound in water at 25°C. Generally, water-soluble drugs are more readily absorbed than lipid-soluble ones. in vitro Caco-2 cell permeability is a crucial measure of drug absorption, with a compound considered to have high Caco-2 permeability if its value surpasses 8 x $10^{-6}$ cm/s. Within the pkCSM model, high Caco-2 permeability aligns with predicted values exceeding 0.90. The intestine typically serves as the primary site for drug absorption from orally administered solutions. A compound with absorbance below 30% is deemed poorly absorbed. An established gauge of blood-brain barrier (BBB) penetration is the log BB ratio, which reflects drug molecule concentrations in the brain and blood. Compounds with log BB > 0.3 exhibit high BBB permeability, while those with log BB < 1.0 show limited BBB distribution. Furthermore, central nervous system (CNS) permeability is a vital parameter for assessing the blood-brain permeability of a drug candidate, expressed as LogPS. Compounds with LogPS <-3 are considered incapable of penetrating the CNS.

Based on these ADME properties, 18 compounds were selected for further analysis. The results for these compounds are detailed in Table 5, while the other parameters are shown in **Table S4** in the supplementary data.

## 6. Docking Validation

Docking validation was performed using AutoDock 4.2. The results are presented in Table 6.

To identify the top CB1 agonist several criteria were taken into account including energy values (e.g. binding energy or Ki values), interactions with key amino acids in the CB1 binding site, number of hydrogen bonds and distances between hydrogen bonds. These interactions are essential for designing effective and selective CB1 agonists.[10] For instance, π-π interactions with aromatic residues (Phe296, Phe170, Phe174, Trp 279) and hydrogen bonds with Ser383 or Thr197 stabilize the agonist-receptor complex, while residues such as Phe379 and Asp366 play a key role in receptor activation

**Table 5. Some ADME parameters of the top-ranked compounds.**

| Code | Water solubility | Caco2 permeability | Intestinal absorption (human) | BBB permeability | CNS permeability | Total Clearance |
|---|---|---|---|---|---|---|
| ZINC17286185 | -5.117 | 0.818 | 83.062 | -0.367 | -2.784 | 0.727 |
| ZINC35562518 | -4.994 | 0.819 | 82.23 | -0.389 | -2.876 | 0.732 |
| ZINC64438506 | -5.467 | 1.165 | 96.008 | -0.435 | -2.363 | 0.804 |
| ZINC64438485 | -5.241 | 1.163 | 97.137 | -0.98 | -2.573 | 0.505 |
| PubChem-121231416 | -4.14 | 0.979 | 94.665 | -0.031 | -2.006 | 0.608 |
| ZINC21797190 | -4.273 | 1.083 | 96.539 | -0.669 | -2.597 | 0.623 |
| PUBChem 157251136 | -4.222 | 1.106 | 94.303 | -0.893 | -2.705 | 1.167 |
| PubChem-42810820 | -5.266 | 1.294 | 94.667 | -0.394 | -1.924 | 0.316 |
| ChemDiv-C260-2692 | -5.941 | 1.284 | 97.247 | -0.422 | -2.392 | 0.819 |
| PubChem-91487881 | -2.946 | 1.374 | 90.351 | -0.966 | -2.226 | 0.369 |
| PubChem-126853168 | -4.351 | 1.428 | 96.515 | -0.399 | -2.234 | 0.514 |
| ZINC65196494 | -4.278 | 1.131 | 98.641 | -0.725 | -2.5 | 0.947 |
| PubChem-41119771 | -4.601 | 1.251 | 95.633 | 0.709 | -1.937 | 0.039 |
| PubChem-3750748 | -5.732 | 1.102 | 91.195 | 0.215 | -1.931 | -0.313 |
| ZINC4034881 | -4.991 | 1.18 | 97.628 | -0.693 | -2.477 | 0.972 |
| PubChem-25352696 | -2.773 | 1.444 | 98.767 | -0.866 | -2.82 | 0.534 |
| PubChem-91428044 | -5.217 | 1.3 | 94.768 | 0.399 | -2.503 | 0.758 |
| ZINC33057775 | -4.528 | 1.202 | 93.212 | -0.615 | -2.241 | -0.075 |

**Table 6. Binding energy (B.E), Intermolecular Energy (I.M.E), Internal Energy (I.E), Torsional Energy (T.E) and constant of inhibition (K.I).**

| Code | B.E (Kcal/mol) | I.M.E (Kcal/mol) | I.E (Kcal/mol) | T.E (Kcal/mol) | KI (nM) |
|---|---|---|---|---|---|
| ChemDiv-C260-2692 | -12.43 | -14.82 | -2.39 | 2.39 | 0.768 |
| PubChem3750748 | -12.3 | -14.69 | -2.05 | 2.39 | 0.958 |
| PubChem25352696 | -10.58 | -12.63 | -1.06 | 1.79 | 17.63 |
| PubChem41119771 | -11.23 | -13.02 | -1.22 | 1.79 | 5.91 |
| PubChem42810820 | -11.6 | -12.79 | -0.77 | 1.19 | 3.13 |
| PubChem91428044 | -10.2 | -12.88 | -1.1 | 2.68 | 33.36 |
| PubChem91487881 | -10.71 | -13.09 | -1.13 | 2.39 | 14.15 |
| PubChem121231416 | -11.63 | -14.32 | -0.86 | 2.68 | 2.98 |
| PubChem126853168 | -12.26 | -13.75 | -0.93 | 1.49 | 1.04 |
| PUBChem157251136 | -11.84 | -14.23 | -1.61 | 2.39 | 2.09 |
| ZINC4034881 | -11.51 | -13.89 | -2.1 | 2.39 | 3.67 |
| ZINC17286185 | -11.41 | -14.39 | -1.84 | 2.98 | 4.36 |
| ZINC21797190 | -12.37 | -14.45 | -1.22 | 2.09 | 0.862 |
| ZINC33057775 | -12.25 | -14.04 | -1.64 | 1.79 | 1.06 |
| ZINC35562518 | -12.22 | -14.9 | -1.74 | 2.68 | 1.11 |
| ZINC64438485 | -13.07 | -15.76 | -1.37 | 2.68 | 0.262 |
| ZINC64438506 | -13.11 | -15.8 | -1.37 | 2.68 | 0.244 |
| ZINC65196494 | -11.7 | -13.49 | -1.28 | 1.79 | 2.65 |

through electrostatic interactions.[10] Based on these criteria three compounds were identified as CB1 receptor agonists: ZINC64438506, ZINC64438485 and PUBChem157251136.

**ZINC64438506:** The docking analysis of CB1 receptor and ZINC64438506 selected agonist is shown in Table 7 and Figure 4. The ZINC64438506 agonist was fixed in the CB1 binding pocket (cavity size = 2963 Å) through various type of interactions, including hydrogen bonds with key amino-acid residues SER A: 173 and SER A: 383, hydrophobic interactions with residues PHE A: 108, PHE A: 177, PHE A: 189, LEU A: 193, THR A: 197, PHE A: 268, TYR A: 275, LEU A: 276, TRP A: 279 and PHE A: 379 and π-π interaction with PHE A: 268. These interactions likely contribute to the compound's low binding affinity (-13.11 Kcal/mol) and low inhibition constant (Ki = 0.244 nM) (Table 6). The strong binding affinity may be attributed to the presence of short hydrogen bonds with SER A: 173 (3.34 Å) and SER A: 383 (51.79 Å).

**ZINC64438485:** The docking analysis of CB1 receptor and ZINC64438485 selected agonist is shown in Table 7 and Figure 5. The ZINC64438485 agonist was fixed in the CB1 binding pocket (cavity size = 2963 Å) through various type of interactions, including hydrogen bonds with key amino-acid residues THR A: 197 and SER A: 383, hydrophobic interactions with residues PHE A: 174, PHE A: 177, PHE A: 189, LEU A: 193, VAL A: 196 and ILE A: 271 and π-π interaction with PHE A: 174, HIS A: 178, PHE A: 268 and TRP A: 279. These interactions likely contribute to the compound's low binding affinity (-13.07 Kcal/mol) and low inhibition constant (Ki = 0.262 nM) (Table 6). The strong binding affinity may be attributed to the presence of short hydrogen bonds with THR A: 197 (1.94 Å) and SER A: 383 (3.08 Å).

**PUBChem-157251136:** The docking analysis of CB1 receptor and PUBChem-157251136 selected agonist is shown in Table 7 and Figure 6. The PUBChem157251136 agonist was fixed in the CB1 binding pocket (cavity size = 2963 Å) through various type of interactions, including hydrogen bonds with key amino-acid residues SER A: 173, HIS A: 178 and SER A: 383, hydrophobic interactions with residues PHE A: 174, PHE A: 177, LEU A: 193, THR A: 197, PHE A: 268, LEU A: 276, TRP A: 279 and PHE A: 379 and π-π interaction with PHE A: 268 and TRP A: 279. These molecular interactions likely contribute to the compound's low binding affinity (-11.84 Kcal/mol) and low inhibition constant (Ki = 2.09 nM) (Table 6). The strong binding affinity may be attributed to the presence of three hydrogen bonds with SER A: 173 (3.23 Å), HIS A: 178 (1.94 Å) and SER A: 383 (2.04Å).

**Table 7.** **Ligand-receptor interactions of the three highest-ranked agonists.**

| Hydrophobic interactions | | | Hydrogen Bonds | | | | $\pi$-Stacking | | | Halogen Bonds | | |
|---|---|---|---|---|---|---|---|---|---|---|---|---|
| Residue | AA | Distance | Residue | AA | Distance H-A | Distance D-A | Residue | AA | Distance (Å) | Residue | AA | Distance |
| 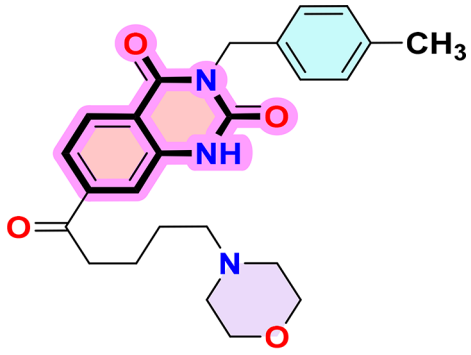 PUBChem 157251136 | | | | | | | | | | | | |
| 174A | PHE | 3.83 | 173A | SER | 3.23 | 3.72 | 268A | PHE | 4.71 | | | |
| 174A | PHE | 3.70 | 178A | HIS | 1.94 | 2.93 | 279A | TRP | 3.94 | | | |
| 177A | PHE | 3.26 | 383A | SER | 2.04 | 2.81 | | | | | | |
| 193A | LEU | 3.37 | | | | | | | | | | |
| 197A | THR | 3.13 | | | | | | | | | | |
| 268A | PHE | 3.48 | | | | | | | | | | |
| 276A | LEU | 3.98 | | | | | | | | | | |
| 279A | TRP | 3.60 | | | | | | | | | | |
| 379A | PHE | 3.49 | | | | | | | | | | |

**Table 7.** *Continued*

| Hydrophobic interactions | | | Hydrogen Bonds | | | | π-Stacking | | | Halogen Bonds | | |
|---|---|---|---|---|---|---|---|---|---|---|---|---|
| Residue | AA | Distance | Residue | AA | Distance H-A | Distance D-A | Residue | AA | Distance (Å) | Residue | AA | Distance |
| 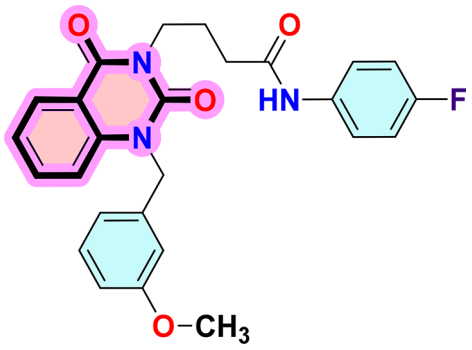 **ZINC64438485** | | | | | | | | | | | | |
| 174A | PHE | 3.87 | 197A | THR | 1.94 | 2.93 | 174A | PHE | 5.09 | | | |
| 177A | PHE | 3.68 | 383A | SER | 3.08 | 3.74 | 178A | HIS | 4.62 | | | |
| 177A | PHE | 3.37 | | | | | 268A | PHE | 4.77 | | | |
| 177A | PHE | 3.88 | | | | | 279A | TRP | 4.93 | | | |
| 189A | PHE | 3.58 | | | | | | | | | | |
| 193A | LEU | 3.42 | | | | | | | | | | |
| 193A | LEU | 3.81 | | | | | | | | | | |
| 196A | VAL | 3.19 | | | | | | | | | | |
| 271A | ILE | 3.91 | | | | | | | | | | |
| 276A | LEU | 3.40 | | | | | | | | | | |
| 279A | TRP | 3.65 | | | | | | | | | | |
| 279A | TRP | 3.77 | | | | | | | | | | |
| 379A | PHE | 3.95 | | | | | | | | | | |
| 379A | PHE | 3.40 | | | | | | | | | | |
| 380A | ALA | 3.34 | | | | | | | | | | |



F1000Research 2025, 14:1322 Last updated: 30 DEC 2025

**Table 7.** *Continued*

| Hydrophobic interactions | | | Hydrogen Bonds | | | | π-Stacking | | | Halogen Bonds | | |
|---|---|---|---|---|---|---|---|---|---|---|---|---|
| Residue | AA | Distance | Residue | AA | Distance H-A | Distance D-A | Residue | AA | Distance (Å) | Residue | AA | Distance |
| 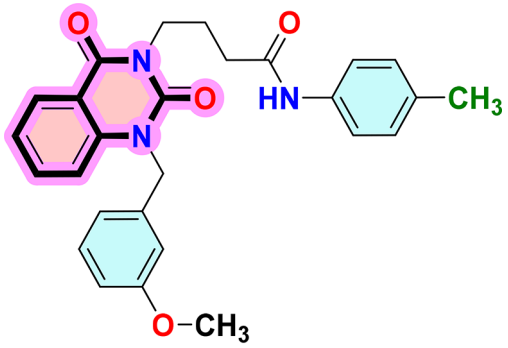 **ZINC64438506** | | | | | | | | | | | | |
| 108A | PHE | 3.77 | 173A | SER | 3.34 | 3.82 | 268A | PHE | 4.77 | | | |
| 177A | PHE | 3.82 | 383A | SER | 1.79 | 2.67 | | | | | | |
| 177A | PHE | 3.22 | | | | | | | | | | |
| 177A | PHE | 3.47 | | | | | | | | | | |
| 189A | PHE | 3.22 | | | | | | | | | | |
| 193A | LEU | 3.47 | | | | | | | | | | |
| 197A | THR | 3.59 | | | | | | | | | | |
| 268A | PHE | 3.63 | | | | | | | | | | |
| 275A | TYR | 3.13 | | | | | | | | | | |
| 276A | LEU | 3.26 | | | | | | | | | | |
| 279A | TRP | 3.40 | | | | | | | | | | |
| 279A | TRP | 3.71 | | | | | | | | | | |
| 279A | TRP | 3.25 | | | | | | | | | | |
| 279A | TRP | 3.56 | | | | | | | | | | |
| 379A | PHE | 3.76 | | | | | | | | | | |



F1000Research 2025, 14:1322 Last updated: 30 DEC 2025

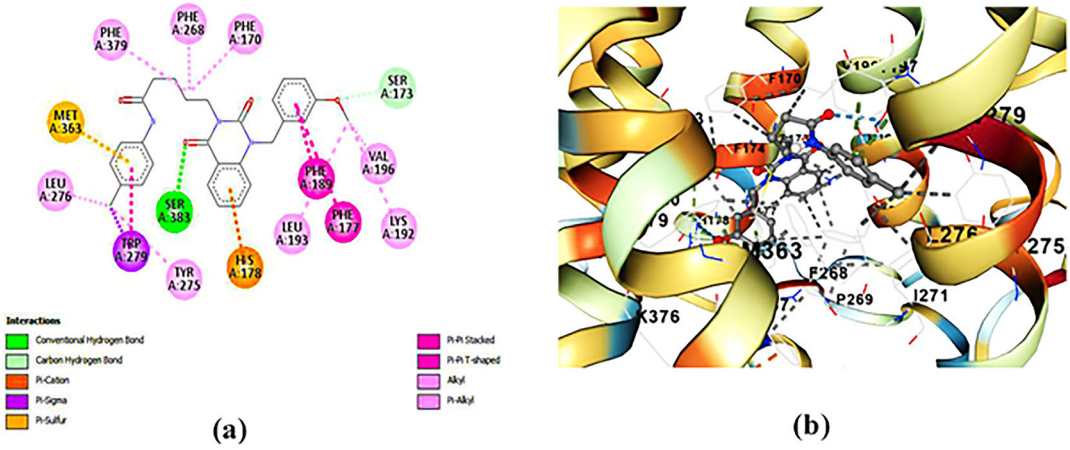


**Figure 4. Docking analysis of ZINC64438506 agonist with CB1 receptor.** (a) 2D view of binding site interactions (b) 3D view of binding conformation.

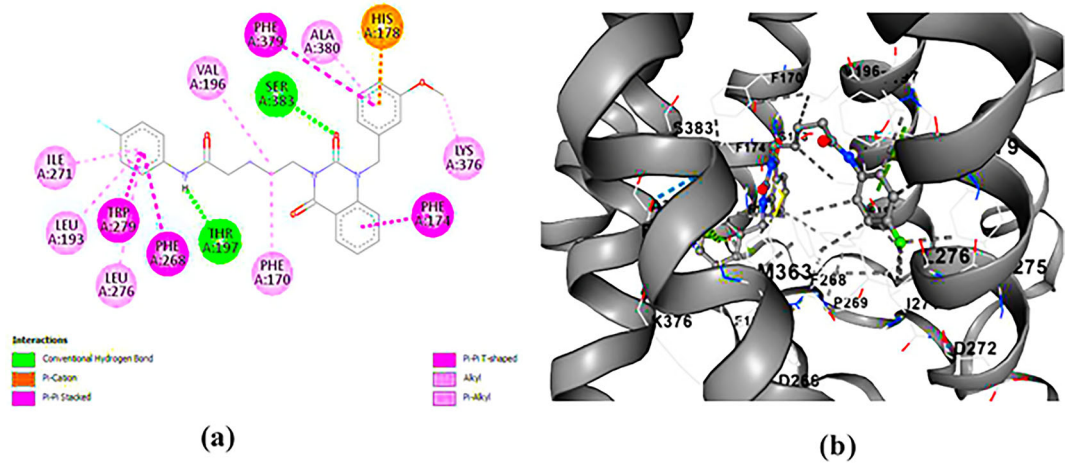


**Figure 5. Docking analysis of ZINC64438485 agonist with CB1 receptor.** (a) 2D view of binding site interactions (b) 3D view of binding conformation.

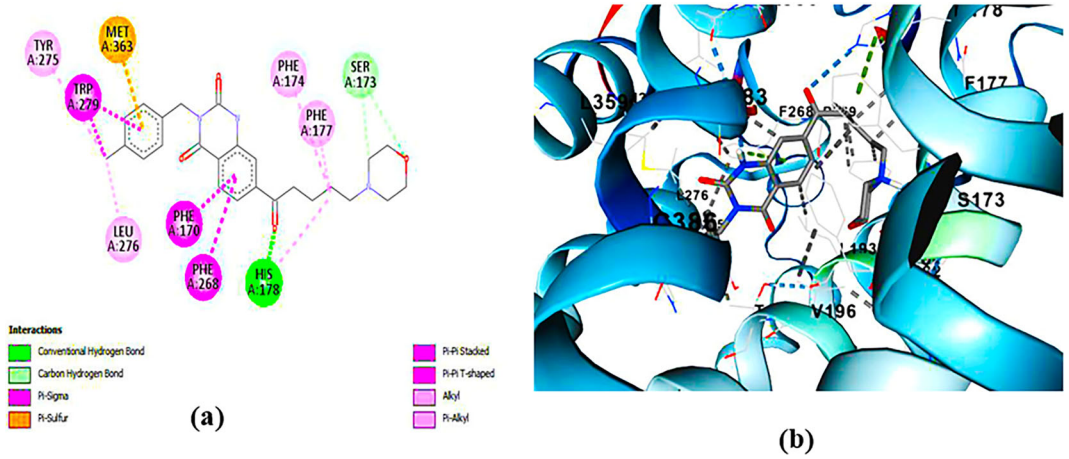


**Figure 6. Docking analysis of PUBChem_157251136 agonist with CB1 receptor.** (a) 2D view of binding site interactions (b) 3D view of binding conformation.

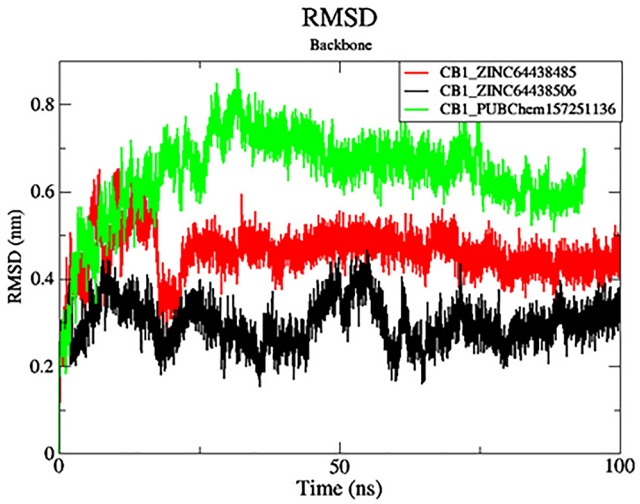


**Figure 7. Plots of RMSD over the 100 ns MD simulation.** The black color was the CB1_ZINC64438506 complex, the red was the CB1_ZINC64438485 complex and the green was the CB1_PUBChem157251136 complex.

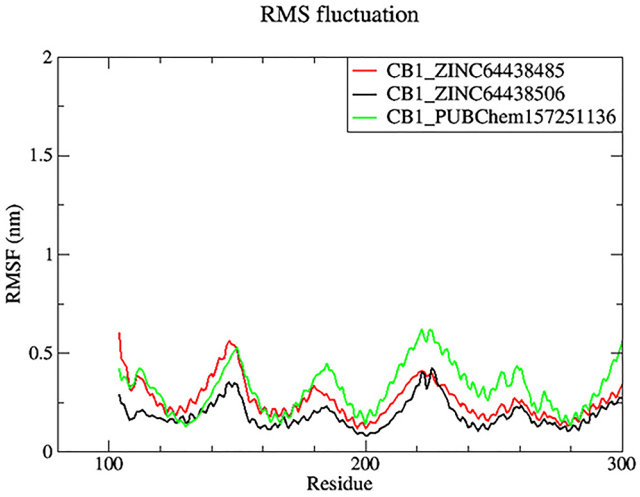


**Figure 8. Plots of RMSF over the 100 ns MD simulation.** The black color was the CB1_ZINC64438506 complex, the red was the CB1_ZINC64438485 complex and the green was the CB1_PUBChem157251136 complex.

## 7. MD simulations

While molecular docking analyses are enough to understand possible bindings based on ligand positioning and receptor-ligand interactions, it should be noted that such methodologies evaluate the flexibility of the ligand only while keeping the protein in a rigid form. Thus, in order to evaluate the best-docked candidates for binding pose stability and dynamics of protein conformation, molecular dynamics (MD) simulations were performed over 100 ns. The results of the MD simulations, including root-mean-square deviation (RMSD), root-mean-square fluctuation (RMSF), and Ligand-Receptor Interaction Plot analyses, can be found in Figures 7–10. These studies provide insights into the dynamic behavior and stability of the protein–ligand complexes over time.

### 7.1 Root Mean Square Deviation (RMSD)

RMSD analysis was carried out for the protein backbone to have an idea of each protein-ligand complex's structural stability during the simulation.[32,33] The results are shown in Figure 7. As shown in Figure 7, mean RMSD values for the CB1_ZINC64438506, CB1_ZINC64438485 and CB1_PUBChem157251136 complex are 0.29 nm, 0.45 nm and 0.64 nm, respectively. The global RMSD values for CB1_ZINC64438506, CB1_ZINC64438485 are small which indicates that these ligands remain stable during the simulation of 100 ns and remained in the binding pocket of the CB1

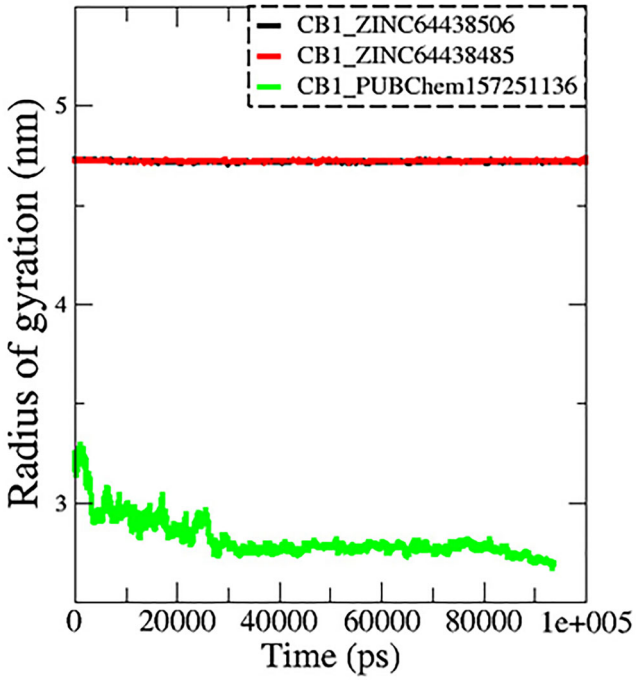


**Figure 9. Plots of Rg during the 100 ns of MD simulation.** The black color represents the CB1_ZINC64438506 complex, the red color represents the CB1_ZINC64438485 complex and the green color represents the CB1_PUBChem157251136 complex.

receptor. The stability of the ligands can be attributed to several strong hydrogen bonds being mediated between these agonists and some of the key amino acids positioned within the binding pocket of the CB1 receptor.

### 7.2 Root mean square fluctuation (RMSF)

Root mean square fluctuation (RMSF) was used to determine the rigid and flexible regions of the CB1 receptor over the 100 ns of MD simulations.[14] RMSF has been term definition, instead of just RMSD values, so that the maximum range of motion of a bound ligand can be seen. RMSF is defined as a standard measure of deviation of a molecule from its initial position.[34] Molecules and residues should not present a high value, which indicates a flexibility, and those that appears low value has a greater rigidity. The RMSF plot for all complexes (Figure 8) indicates that most residues located in the CB1 receptor has a low RMSF value, indicating they were rigid and retained stability over the entire 100 ns MD simulation.

### 7.3 Radius of gyration (Rg)

The radius of gyration (Rg) is another important metric measured during MD simulations to determine spatial characteristics of a protein-ligand complex. The radius of gyration is the root mean square distance of all atoms making up a given structure from a relative center common point (the center of mass) and signifies extension versus folding of the given structure. Therefore, a lower Rg would imply stability and a more tightly folded structure, while a higher Rg would imply extension and flexibility of possible structures. In this work, the Rg profiles remained stable over the course of 100 ns of MD simulation for the complexes CB1_ZINC64438506 (mean = 4.70 nm; Figure 9) and CB1_ZINC64438485 (mean = 4.72 nm), while the complex CB1_PUBChem157251136 decreased in Rg (mean = 2.81 nm).

### 7.4 Hydrogen bonds

One of the main factors influencing the affinity of a molecule for the protein binding pocket is its ability to form and maintain hydrogen bonds with the binding site residues. The stability of the selected agonist was assessed by analyzing the hydrogen bonds between the ligand and the protein. The results are presented in Figure 10.

Compounds ZINC64438506, ZINC64438485, and PUBChem157251136 form two, two and three hydrogen bonds with the CB1 binding site, respectively, indicating strong and specific interactions with the protein. These results are consistent with the docking results.

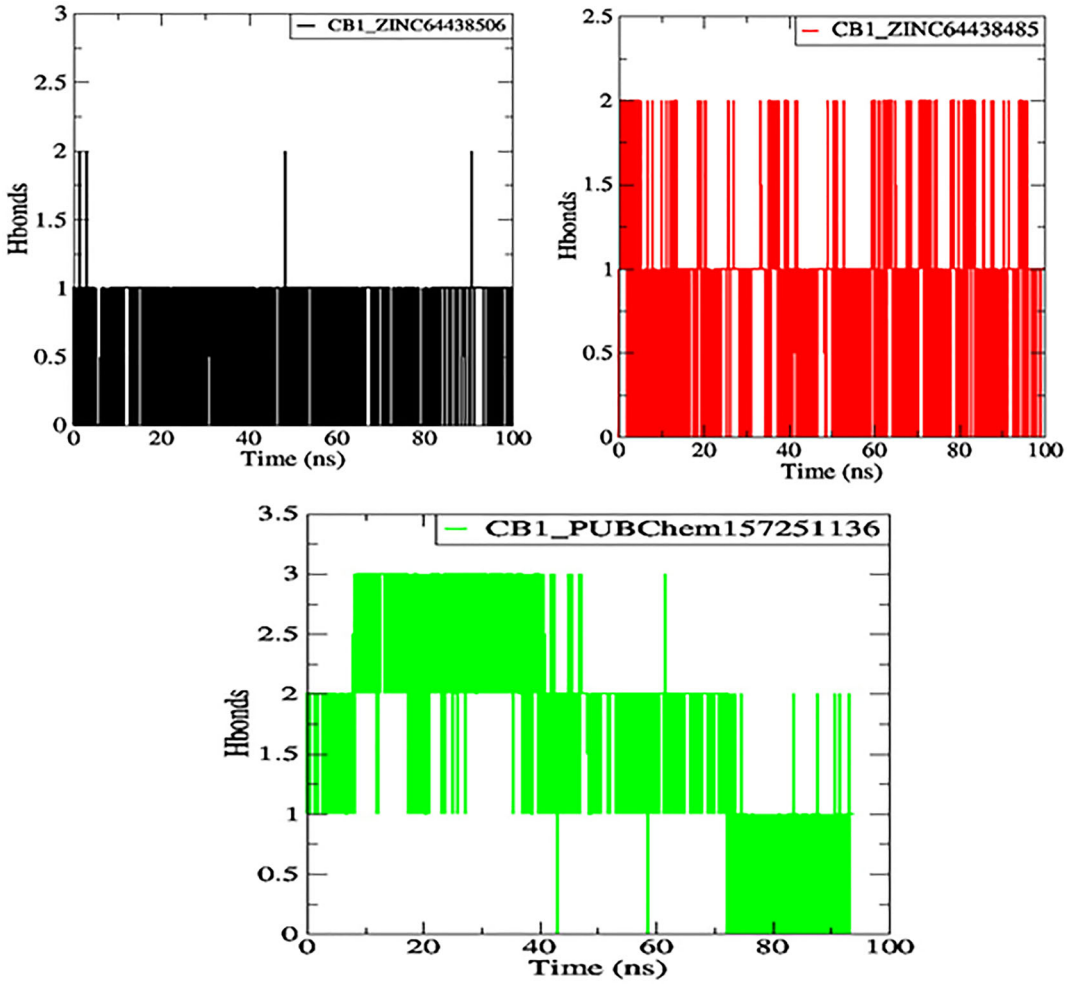


**Figure 10. Plot of H-bonds during the 100 ns of MD simulation.** The black color represents the CB1_ZINC64438506 complex, the red color represents the CB1_ZINC64438485 complex and the green color represents the CB1_PUBChem157251136 complex.

## 8. MM-GBSA calculation for the top three ranked compounds

The binding free energy of all complexes was calculated to revalidate the binding affinity obtained from molecular docking analysis. The results are presented in Table 8. A $\Delta G_{bind}$ value below -7 Kcal/mol indicates strong binding, a value between -5 and -7 kcal/mol suggests moderate binding, and a value between -2 and -5 kcal/mol corresponds to weak binding.[35] The results show that all the agonists exhibit exceptionally low binding free energies, indicating a remarkable affinity for the target protein.

The results also highlight the crucial role of Van der Waals and electrostatic interactions in mediating protein-ligand binding throughout the molecular dynamics simulations (Figure 11).

**Table 8. MM-GBSA calculations for the top three ranked compounds.**

| Complex | $\Delta G_{GAS}$ (Kcal/mol) | $\Delta G_{SOLV}$ (Kcal/mol) | $\Delta G_{bind}$ (Kcal/mol) |
|---|---|---|---|
| CB1_ZINC64438506 | -80.76 | 30.99 | -49.77 |
| CB1_PUBChem157251136 | -107.10 | 76.51 | -30.59 |
| CB1_ZINC64438485 | -82.29 | 32.31 | -49.98 |

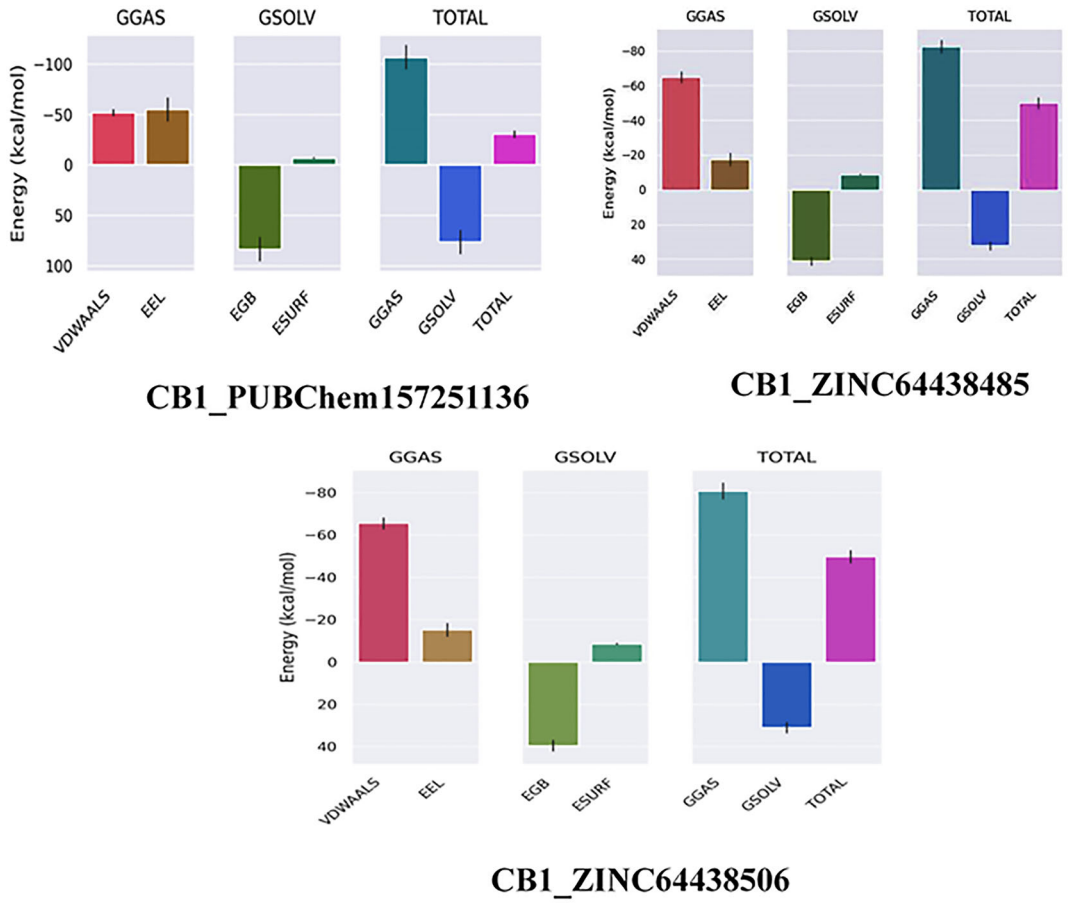


**Figure 11. Binding free energy plot of the three highest ranked agonists.**

## 9. Quinazoline-2,4(1H,3H)-dione derivatives

Quinazoline-2,4(1H,3H)-dione derivatives represent a highly promising class of heterocyclic compounds with broad therapeutic potential, particularly as anticancer,[36–38] antibacterial,[39,40] antihypertensive,[41] phosphodiesterase (PDE) 4 inhibition,[42] 5-HT3A receptor antagonist,[43] anti-inflammatory,[44] and anan up-and-comingtiviral agents.[45] Their fused benzopyrimidinedione scaffold provides an excellent pharmacophore for targeting key biological pathways (Figure 12). According to the article's findings, quinazoline-2,4(1H,3H)-dione derivatives may be the first of a new class of CB1 agonists.

## 10. Different synthesis routes of substituted quinazoline-2,4-dione scaffold

To synthesise the substituted quinazoline-2,4-dione and the highest-ranking agonists identified by virtual screening, namely ZINC64438506, PUBChem157251136 and ZINC64438485, several plausible synthesis strategies were developed based on established methodologies.[43] These routes use various precursors such as 2-aminobenzoic acid,[44] methyl 2-nitrobenzoate, 2-iodobenzamides[46] or 2H-benzo [d][1,3]oxazine-2,4(1H)-dione[47] (Figure 13). The choice of starting material is guided by both its availability and synthetic feasibility. Depending on the substrate, the desired compounds can be obtained by catalytic transformations, particularly transition metal-catalysed couplings, or by intramolecular cyclisation reactions that form the characteristic quinazoline skeleton. The synthetic flexibility offered by these precursors allows the reaction conditions to be adjusted to optimise yield and purity, making them suitable candidates for further pharmacological evaluation and development.

Translated with DeepL.com (free version)

To synthesise substituted quinazoline-2,4-dione and the top-ranked agonists identified by virtual screening - namely ZINC64438506, PUBChem157251136 and ZINC64438485 - several plausible synthetic strategies have been devised, based on established methodologies.[46] These routes use various precursors such as 2-aminobenzoic acid,[47] methyl 2-nitrobenzoate[48] which undergoes catalytic hydrogenation under mild and green conditions (1 atm of $H_2$ in ethanol at

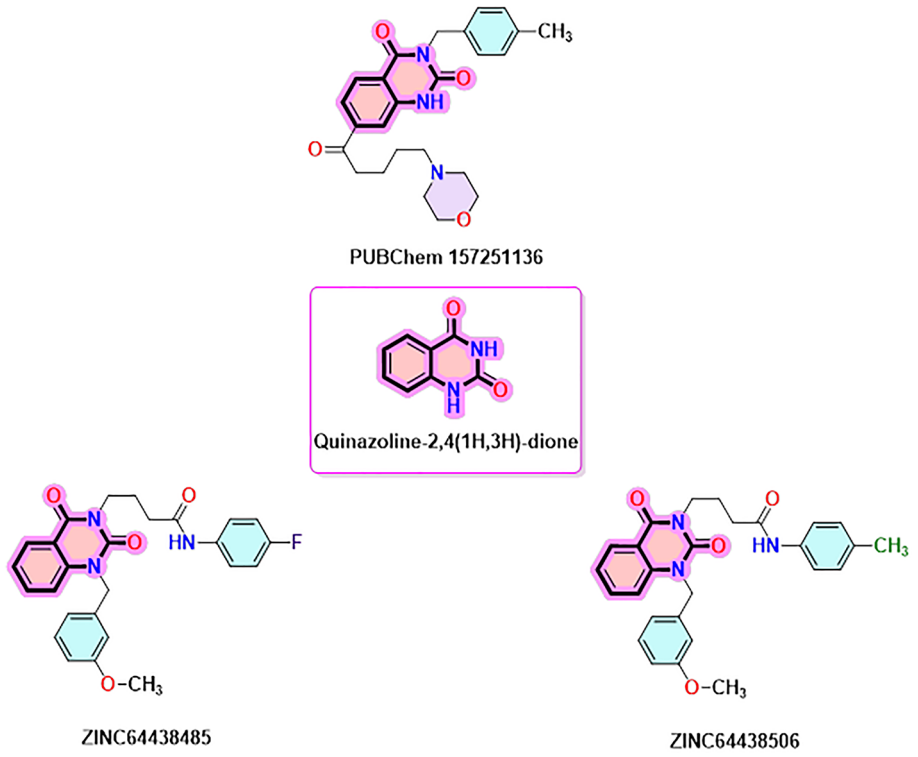


**Figure 12. Quinazoline-1, 4(1H, 3H)-dione scaffold and the three highest-ranked agonists (ZINC64438506, PUBChem157251136 and ZINC64438485).**

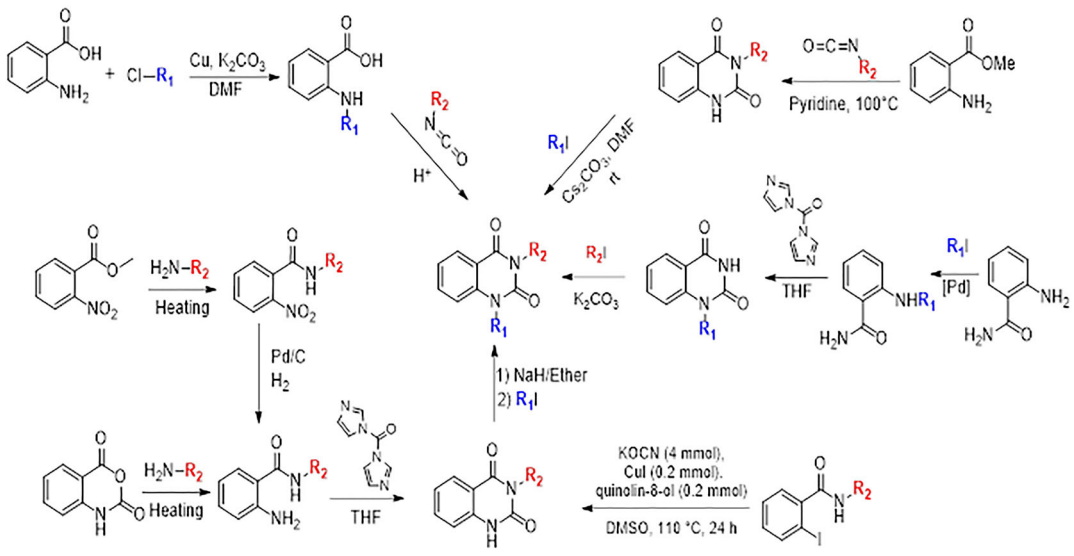


**Figure 13. Different synthesis routes of substituted quinazoline-2, 4-dione.**

room temperature),[49,50] 2-iodobenzamides[51] or 2H-benzo [d][1,3]oxazine-2,4(1H)-dione[52] (Figure 13). The choice of starting material is guided by both availability and synthetic feasibility. Depending on the substrate, the desired compounds can be accessed by catalytic transformations, including transition metal-catalysed couplings, or by intramolecular cyclisation reactions that form the characteristic quinazoline scaffold. The synthetic flexibility offered by these precursors allows reaction conditions to be fine-tuned to optimize yield and purity, making them suitable candidates for further pharmacological evaluation and development.

## IV. Conclusion

In this study, pharmacophore-based virtual screening was conducted to identify the best CB1 agonist based on the pharmacophoric features of AM11542. The optimal pharmacophore model comprised two hydrogen bond acceptors (HBA), one aromatic ring (AR), and two hydrophobic centers (HY). This model was subsequently applied to screen a database of more than five million compounds, including Molprot with 4,742,020 molecules, ChEMBL34 with 2,264,112 molecules, ZINC with 13,127,550 molecules, ChemDiv with 1,456,120 molecules, ChemSpace with 50,181,678 molecules, Enamine with 4,117,328 molecules, MCULE with 39,843,637 molecule, MCULE-ULTIMATE with 126,471,502 molecules, NCI Open Chemical Repository with 52,237 molecules, LabNetwork with 1,794,286 molecules and PubChem with 103,302,052 molecules. Based on the generated pharmacophore model, 433 compounds were selected for further evaluation. Subsequent molecular docking refined this selection to 61 high-affinity ligands (≤-9.00 kcal/mol), which were refined to 18 promising leads through ADME-Tox analysis. Among these, three compounds were selected as potential agonists of the CB1 receptor based on their binding affinity and strong interactions with key binding pocket residues (Ser383, Ser173, His178, and Thr197). Molecular dynamics simulations using Gromacs 2024.4 confirmed the structural stability of these complexes, with low RMSD (<1 nm) and RMSF (<1 nm) values, indicating minimal conformational fluctuations. MM-GBSA calculations further validated the thermodynamic stability, with binding free energies ranging from -30.59 to -49.98 kcal/mol, reinforcing their potential as potent CB1 agonists. The three selected compounds shared a common quinazolinz-2,4(1H,3H)-dione scarfed, indicating that derivatives of this structure could pave the way for developing new CB1 receptor agonists.

## Data availability statement

### Underlying data

No underlying data are associated with this article.

### Extended data

Repository name: "Quinazoline-2,4(1H,3H)-dione derivatives as new class of CB1 Agonists: A ppharmacophore-based virtual screening workflow and Lead discovery" https://doi.org/10.5281/zenodo.17274156.[53]

This project contains the following extended data:

- **Supplementary Table 1**. (Binding free energies of the 433 top-ranked compounds from pharmacophore-based virtual screening)
- **Supplementary Table 2.** (Computationally predicted toxicity profiles of top 61 compounds)
- **Supplementary Table 3.** (Physicochemical properties of studied compounds)
- **Supplementary Table 4.** (Some ADME parameters of the top-ranked compounds)



## References


1. Sugiura T, Kondo S, Sukagawa A, *et al.*: **2-arachidonoylglycerol: A possible endogenous cannabinoid receptor ligand in brain.** *Biochem. Biophys. Res. Commun.* 1995; **215**: 89–97.
PubMed Abstract | Publisher Full Text
2. Howlett AC, Barth F, Bonner TI, *et al.*: **International Union of Pharmacology. XXVII. Classification of Cannabinoid Receptors.** *Pharmacol. Rev.* 2002 Jun 1; **54**(2): 161–202.
PubMed Abstract | Publisher Full Text
3. Lemberger L: **Potential therapeutic usefulness of marijuana.** *Annu. Rev. Pharmacol. Toxicol.* 1980; **20**: 151–172.
Publisher Full Text
4. Li HL: **An Archaeological and Historical Account of Cannabis in China Author (s): Hui-Lin Li Published by: Springer on behalf of New York Botanical Garden Press Stable URL: Accessed: 15-07-2016 23: 13 UTC An Archaeologica.** *Econ. Bot.* 1974; **28**(4): 437–448.
Reference Source
5. Makriyannis A: **2012 division of medicinal chemistry award address. Trekking the cannabinoid road: A personal perspective.** *J. Med. Chem.* 2014; **57**(10): 3891–3911.
PubMed Abstract | Publisher Full Text | Free Full Text
6. Caulfield MP, Brown DA: **Cannabinoid receptor agonists inhibit Ca current in NG108–15 neuroblastoma cells via a Pertussis toxin-sensitive mechanism.** *Br. J. Pharmacol.* 1992; **106**(2): 231–232.
PubMed Abstract | Publisher Full Text | Free Full Text
7. Pryce G, Ahmed Z, Hankey DJR, *et al.*: **Cannabinoids inhibit neurodegeneration in models of multiple sclerosis.** *Brain.* 2003; **126**(10): 2191–2202.
PubMed Abstract | Publisher Full Text
8. Hua T, Vemuri K, Nikas SP, *et al.*: **Crystal structures of agonist-bound human cannabinoid receptor CB 1.** *Nature.* 2017; **547**(7664): 468–471.
PubMed Abstract | Publisher Full Text | Free Full Text
9. Yang X, Wang X, Xu Z, *et al.*: **Molecular mechanism of allosteric modulation for the cannabinoid receptor CB1.** *Nat. Chem. Biol.* 2022; **18**(8): 831–840.
PubMed Abstract | Publisher Full Text

10. Hua T, Vemuri K, Pu M, *et al.*: **Crystal Structure of the Human Cannabinoid Receptor CB1.** *Cell.* 2016; **167**(3): 750–762.e14.
PubMed Abstract | Publisher Full Text | Free Full Text

11. Ramesh K, Rosenbaum DM: **Molecular basis for ligand modulation of the cannabinoid CB1 receptor.** *Br. J. Pharmacol.* 2022; **179**(14): 3487–3495.
PubMed Abstract | Publisher Full Text

12. Editor D: **Cryo-EM structure of cannabinoid receptor CB1- β -arrestin complex.** 2024 (December 2023); 230–4.

13. El Aissouq A, El Chedadi O, Bouachrine M, *et al.*: **Development of novel monoamine oxidase B (MAO-B) inhibitors by combined application of docking-based alignment, 3D-QSAR, ADMET prediction, molecular dynamics simulation, and MM _ GBSA binding free energy.** *J. Biomol. Struct. Dyn.* 2023; **41**(10): 4667–4680.
PubMed Abstract | Publisher Full Text

14. El Aissouq A, Bouachrine M, Ouammou A, *et al.*: **Neuroscience Letters Homology modeling, virtual screening, molecular docking, molecular dynamic (MD) simulation, and ADMET approaches for identification of natural anti-Parkinson agents targeting MAO-B protein.** *Neurosci. Lett.* 2022; **786**(July): 136803.
PubMed Abstract | Publisher Full Text

15. El Aissouq AEL, Bouachrine M, Ouammou A, *et al.*: **Computational investigation of unsaturated ketone derivatives as MAO-B inhibitors by using QSAR, ADME/Tox, molecular docking, and molecular dynamics simulations.** *Turk. J. Chem.* 2022; **46**(3): 687–703.
PubMed Abstract | Publisher Full Text | Free Full Text

16. Enneiymy M, Mohammad-Salim HA, Oubella A, *et al.*: **In-Silico Analysis of Benzo-Selenadiazole Hybrids: Reactivity and Anticancer Potential Assessed Through DFT, Molecular Dynamics, Molecular Docking, and ADMET.** *Polycycl. Aromat. Compd.* 1–23.

17. Bellapukonda SM, Singothu S, Singampalli A, *et al.*: **Exploring spirocyclic isoquinoline-piperidine compounds in tuberculosis therapy: ADMET profiling, docking, DFT, MD simulations, and MMGBSA analysis.** *Comput. Biol. Chem.* 2025 Oct 1; **118**: 108447.
PubMed Abstract | Publisher Full Text

18. Jász Á, Rák Á, Ladjánszki I, *et al.*: **Optimized GPU implementation of Merck Molecular Force Field and Universal Force Field.** *J. Mol. Struct.* 2019; **1188**: 227–233.
Publisher Full Text

19. El Aissouq A, Chedadi O, Bouachrine M, *et al.*: **Identification of Novel SARS-CoV-2 Inhibitors: A Structure-Based Virtual Screening Approach.** *J. Chem.* 2021; **2021**: 1–7.
Publisher Full Text

20. Páll S, Abraham MJ, Kutzner C, *et al.*: **Tackling exascale software challenges in molecular dynamics simulations with GROMACS.** *Lecture Notes in Computer Science (including subseries Lecture Notes in Artificial Intelligence and Lecture Notes in Bioinformatics).* 2015; **8759**: 3–27.
Publisher Full Text

21. Buslaev P, Groenhof G: **gmXtal: Cooking Crystals with GROMACS.** *Protein J.* 2024; **43**(2): 200–206.
PubMed Abstract | Publisher Full Text | Free Full Text

22. Typing A of the CGFF (CGenFF) IBP and A: **CHARMM General Force Field (CG).** *J. Comput. Chem.* 2010; **31**(4): 671–690.
PubMed Abstract | Publisher Full Text

23. Zoete V, Cuendet MA, Grosdidier A, *et al.*: **SwissParam: A fast force field generation tool for small organic molecules.** *J. Comput. Chem.* 2011; **32**(11): 2359–2368.
PubMed Abstract | Publisher Full Text

24. Altharawi A, Enneiymy M, Elmachkouri YA, *et al.*: **Synthesis, characterization, DFT, and *in-Silico* analysis of isoxazole-thiazolidinone hybrids: Reactivity and anticancer potential assessed through pharmacological network, molecular dynamics, molecular docking, and ADMET analysis.** *J. Mol. Struct.* 2025 Aug 5; **1336**: 142088.
Publisher Full Text

25. Šali A, Blundell TL: **Comparative protein modelling by satisfaction of spatial restraints.** *J. Mol. Biol.* 1993; **234**: 779–815.
PubMed Abstract | Publisher Full Text

26. Sunseri J, Koes DR: **Pharmit: interactive exploration of chemical space.** *Nucleic Acids Res.* 2016; **44**(W1): W442–W448.
PubMed Abstract | Publisher Full Text | Free Full Text

27. Lipinski CA, Lombardo F, Dominy BW, *et al.*: **Experimental and computational approaches to estimate solubility and permeability in drug discovery and development settings.** *Adv. Drug Deliv. Rev.* 2012; **64**(SUPPL): 4–17.
Publisher Full Text

28. Feng X: **Study on numbers of multi-tooth meshing teeth pairs for involute internal gear pairs with small tooth number difference.** *Adv. Mater. Res.* 1998; **655-657**(Cmc): 578–585.
Publisher Full Text

29. Veber DF, Johnson SR, Cheng HY, *et al.*: **Molecular properties that influence the oral bioavailability of drug candidates.** *J. Med. Chem.* 2002; **45**(12): 2615–2623.
Publisher Full Text

30. Enyedy IJ, Egan WJ: **Can we use docking and scoring for hit-to-lead optimization?** *J. Comput. Aided Mol. Des.* 2008; **22**(3–4): 161–168.
Publisher Full Text

31. Guex N, Peitsch MC: **SWISS-MODEL and the Swiss-PdbViewer: An environment for comparative protein modeling.** *Electrophoresis.* 1997; **18**(15): 2714–2723.
PubMed Abstract | Publisher Full Text

32. Elhady SS, Abdelhameed RFA, Rania MT, *et al.*: **Molecular Docking and Dynamics Simulation Study of.** *Mdpi.* 2021.

33. Enneiymy M, El Aissouq A: **Carvacrol-Derived 1,2,3-Triazole Hybrids: Synthesis, Computational Insights, and Targeted Inhibition of EGFR, BRAF V600E, and Tubulin Enzymes.** *J. Fluoresc.* 2025.
PubMed Abstract | Publisher Full Text

34. Swetha RG, Ramaiah S, Anbarasu A: **Molecular Dynamics Studies on D835N Mutation in FLT3 - Its Impact on FLT3 Protein Structure.** *J. Cell. Biochem.* 2016; **117**(6): 1439–1445.
PubMed Abstract | Publisher Full Text

35. Valdés-Tresanco MS, Valdés-Tresanco ME, Valiente PA, *et al.*: **Gmx_MMPBSA: A New Tool to Perform End-State Free Energy Calculations with GROMACS.** *J. Chem. Theory Comput.* 2021; **17**(10): 6281–6291.
PubMed Abstract | Publisher Full Text

36. Betti M, Genesio E, Panico A, *et al.*: **Process development and scale-up for the preparation of the 1-methyl-quinazoline-2,4-dione wnt inhibitor SEN461.** *Org. Process. Res. Dev.* 2013; **17**(8): 1042–1051.
Publisher Full Text

37. El-Deeb IM, Bayoumi SM, El-Sherbeny MA, *et al.*: **Synthesis and antitumor evaluation of novel cyclic arylsulfonylureas: ADME-T and pharmacophore prediction.** *Eur. J. Med. Chem.* 2010; **45**(6): 2516–2530.
PubMed Abstract | Publisher Full Text

38. Park Choo HY, Kim M, Lee SK, *et al.*: **Solid-phase combinatorial synthesis and cytotoxicity of 3-aryl-2,4-quinazolindiones.** *Bioorganic and Medicinal Chemistry.* 2002; **10**(3): 517–523.
PubMed Abstract | Publisher Full Text

39. German N, Malik M, Rosen JD, *et al.*: **Use of gyrase resistance mutants to guide selection of 8-methoxy- quinazoline-2,4-diones.** *Antimicrob. Agents Chemother.* 2008; **52**(11): 3915–3921.
PubMed Abstract | Publisher Full Text | Free Full Text

40. Malik M, Marks KR, Mustaev A, *et al.*: **Fluoroquinolone and quinazolinedione activities against wild-type and gyrase mutant strains of Mycobacterium smegmatis.** *Antimicrob. Agents Chemother.* 2011; **55**(5): 2335–2343.
PubMed Abstract | Publisher Full Text | Free Full Text

41. Hedner T, Persson B, Berglund G: **Ketanserin, a novel 5-hydroxytryptamine antagonist: monotherapy in essential hypertension.** *Br. J. Clin. Pharmacol.* 1983; **16**(2): 121–125.
PubMed Abstract | Publisher Full Text | Free Full Text

42. Redondo M, Zarruk JG, Ceballos P, *et al.*: **Neuroprotective efficacy of quinazoline type phosphodiesterase 7 inhibitors in cellular cultures and experimental stroke model.** *Eur. J. Med. Chem.* 2012; **47**(1): 175–185.
PubMed Abstract | Publisher Full Text

43. Lee BH, Choi MJ, Jo MN, *et al.*: **Quinazolindione derivatives as potent 5-HT3A receptor antagonists.** *Bioorganic and Medicinal Chemistry.* 2009; **17**(13): 4793–4796.
PubMed Abstract | Publisher Full Text

44. Gupta T, Rohilla A, Pathak A, *et al.*: **Current perspectives on quinazolines with potent biological activities: A review.** *Synth. Commun.* 2018; **48**(10): 1099–1127.
Publisher Full Text

45. Kang D, Zhang H, Zhou Z, *et al.*: **First discovery of novel 3-hydroxy-quinazoline-2,4(1H,3H)-diones as specific anti-vaccinia and adenovirus agents via 'privileged scaffold' refining approach.** *Bioorg. Med. Chem. Lett.* 2020; **26**(January): 5182–5186.
Publisher Full Text

46. Gheidari D, Mehrdad M, Maleki S: **The quinazoline-2,4(1H,3H)-diones skeleton: A key intermediate in drug synthesis.** *Sustain. Chem. Pharm.* 2022; **27**(March): 100696.
Publisher Full Text

47. Bailey J, Oliveri A, Levin E: **NIH Public Access.** *Bone.* 2013; **23**(1): 1–7.

48. Klenc J, Raux E, Barnes S, *et al.*: **Synthesis of 4-Substituted 2- (4-Methylpiperazino) pyrimidines and Quinazoline Analogs as Serotonin 5-HT 2A Receptor Ligands.** *J. Heterocyclic Chem.* 2009; **46**(November): 1259–1265.
Publisher Full Text

49. Enneiymy M, Fioux P, Le Drian C, *et al.*: **Palladium nanoparticles embedded in mesoporous carbons as efficient, green and reusable catalysts for mild hydrogenations of nitroarenes.** *RSC Adv.* 2020; **10**(60): 36741–36750.
PubMed Abstract | Publisher Full Text | Free Full Text

50. Enneiymy M, Le Drian C, Becht JM: **Green reusable Pd nanoparticles embedded in phytochemical resins for mild hydrogenations of nitroarenes.** *New J. Chem.* 2019; **43**(44): 17383–17389.
Publisher Full Text

51. Nasirpour A, Ghasemi Z, Hosseini-Yazdi SA, *et al.*: **Synthesis of N3-substituted-quinazoline-2,4(1H,3H)-diones via CuI-catalyzed coupling of 2-iodobenzamides with potassium cyanate.** *Results in Chemistry.* 2025; **15**(March): 102204.
Publisher Full Text

52. Clark RL, Clements CJ, Barrett MP, *et al.*: **Identification and development of the 1,4-benzodiazepin-2-one and quinazoline-2,4-dione scaffolds as submicromolar inhibitors of HAT.** *Bioorganic and Medicinal Chemistry.* 2012; **20**(20): 6019–6033.
PubMed Abstract | Publisher Full Text

53. Aissouq EL, Abdellah Stitou M, Enneiymy M, *et al.*: **Quinazoline-2, 4 (1H, 3H) -dione derivatives as new class of CB1 Agonists: A ppharmacophore-based virtual screening workflow and Lead discovery.** *Zendo.* 2025; **4**.

# Open Peer Review

## Current Peer Review Status: ✔ ✔

**Version 1**

Reviewer Report 30 December 2025

https://doi.org/10.5256/f1000research.189041.r439371



✔ **Mourad Fawzi**
Faculty of Sciences Semlalia, Cadi Ayyad University, Department of Chemistry, Laboratory of Molecular Chemistry, Marrakech, Morocco

The study entitled "***Quinazoline-2,4(1H,3H)-dione derivatives as new class of CB1 Agonists: A pharmacophore-based virtual screening workflow and Lead discovery***" presents a pharmacophore-based virtual screening of a large database aimed at developing new CB1 agonists. I believe this work is suitable for publication in ***F1000 Research*** before the minor revisions below:

**Comments for the authors:**

1. Page 17: "form two, two and three hydrogen bonds with the CB1 binding site, respectively, ..." – The word "two" is repeated; please remove one.
2. Some abbreviations are not clearly defined in the manuscript, such as **GPCR** and **ICL3**. Please ensure all abbreviations are spelled out upon first use.
3. Page 19: The sentence "Translated with DeepL.com (free version)" should be removed.
4. More details about the advantage of work in conclusion are required
5. Grammatical errors and typos are present throughout the manuscript. A thorough proofreading is recommended to improve clarity and language quality.
6. Regarding **Table 6**: The reported $\mathbf{K_i}$ values indicate that the screened compounds exhibit promising drug-like properties. Therefore, I suggest modifying the title to better reflect this finding. Proposed revision:

" ***Quinazoline-2,4(1H,3H)-dione derivatives as new class of CB1 Agonists: A pharmacophore-based virtual screening workflow and Lead discovery*** "

**Is the work clearly and accurately presented and does it cite the current literature?**
Yes

**Is the study design appropriate and is the work technically sound?**
Yes

**Are sufficient details of methods and analysis provided to allow replication by others?**

Yes

**If applicable, is the statistical analysis and its interpretation appropriate?**
I cannot comment. A qualified statistician is required.

**Are all the source data underlying the results available to ensure full reproducibility?**
No source data required

**Are the conclusions drawn adequately supported by the results?**
Partly

***Competing Interests:*** No competing interests were disclosed.

***Reviewer Expertise:*** Bioinformatics, Organic Chemistry, Medicinal Chemistry

**I confirm that I have read this submission and believe that I have an appropriate level of expertise to confirm that it is of an acceptable scientific standard.**

Reviewer Report 29 December 2025

https://doi.org/10.5256/f1000research.189041.r437306



**Fatima En-nahli**
University of Moulay Ismail, Meknes, Morocco

Dear Editor,
I would like to thank you for the opportunity to review the manuscript entitled *"Quinazoline-2,4(1H,3H)-dione derivatives as a new class of CB1 Agonists: A pharmacophore-based virtual screening workflow and Lead discovery."* The study addresses a relevant topic and provides valuable insights into CB1 agonist identification through an in silico workflow. Overall, the manuscript is promising; however, I believe that **minor revisions** are required to improve clarity and scientific rigor.
Please find below my main remarks for the authors:

1. The current title would benefit from being reformulated to make it more concise and more attractive to readers. A clearer title highlighting the novelty and the integrated workflow is recommended.
2. The authors mention the use of molecular dynamics (MD) simulations in the Materials and Methods section, but MD is not mentioned in the Abstract. For coherence and completeness, this important component of the workflow should be briefly stated in the Abstract.
3. In the graphical abstract, the authors indicate two docking steps (first using AutoDock Vina, then AutoDock4). It would be helpful to briefly clarify the rationale behind this double-docking strategy and how each tool contributes to the screening workflow.
4. The authors are encouraged to integrate a comparative discussion between the

pharmacophore hits, docking scores, and the stability of key amino acids involved in ligand recognition, supported by MD fluctuation analysis (e.g., RMSF). This would reinforce the consistency and predictive power of the multi-step in silico approach.

5. Since none of the proposed candidates were synthesized or experimentally validated, the authors should clearly state the value of the in silico-only approach and discuss its limitations. It is also recommended to suggest potential collaboration with experimental researchers for future synthesis and biological evaluation.
6. Given that the identified compounds appear to be promising drug candidates, it would be appropriate to add a short section in the conclusion outlining perspectives for future work.

Overall, the manuscript represents an interesting contribution, and after addressing these minor points, it will be suitable for publication.
Thank you again for entrusting me with the review of this manuscript.
Kind regards,

**Is the work clearly and accurately presented and does it cite the current literature?**
Yes

**Is the study design appropriate and is the work technically sound?**
Yes

**Are sufficient details of methods and analysis provided to allow replication by others?**
Yes

**If applicable, is the statistical analysis and its interpretation appropriate?**
Yes

**Are all the source data underlying the results available to ensure full reproducibility?**
Yes

**Are the conclusions drawn adequately supported by the results?**
Yes

***Competing Interests:*** No competing interests were disclosed.

***Reviewer Expertise:*** chimie informatique

**I confirm that I have read this submission and believe that I have an appropriate level of expertise to confirm that it is of an acceptable scientific standard.**